Spin splitting of electron states in (110) quantum wells: Symmetry analysis and k·p theory versus microscopic calculations

M. O. Nestoklon and S. A. Tarasenko
Ioffe Physical-Technical Institute, Russian Academy of Sciences, St. Petersburg 194021, Russia

J.-M. Jancu
FOTON-INSA Laboratory, UMR 6082 au CNRS, INSA de Rennes, 35043 Rennes Cedex, France

P. Voisin
CNRS-Laboratoire de Photonique et de Nanostructures, 91460 Marcoussis, France

(Received 23 March 2012; published 9 May 2012)

Spin splittings in quantum wells have attracted considerable attention over the past decade due to potential application of semiconductor spin properties to "spintronic devices." Recent experimental results stimulate theoretical investigations of new physical situations like unconventional growth directions. Here we focus on electron spin properties in (110)-oriented quantum wells that are of particular interest because qualitative symmetry analysis shows that spin relaxation by the D'yakonov-Perel' mechanism should be strongly suppressed in this geometry. We combine symmetry analysis, envelope function theory, and tight-binding calculation and obtain quantitative description of the in-plane wave vector, well width, and applied electric field dependence of the spin structure of electron subbands in (110) quantum wells.

DOI: 10.1103/PhysRevB.85.205307 PACS number(s): 75.70.Tj, 73.21.Fg, 72.25.Rb

I. INTRODUCTION

Spin-orbit coupling in semiconductor low-dimensional structures has been attracting much attention since it allows one to manipulate the spins of charge carriers by affecting their orbital motion.[1,2] A remarkable consequence of spin-orbit coupling is the splitting of electron states in the absence of external magnetic field. In quantum wells (QWs) this splitting is linear in the in-plane wave vector $\boldsymbol{k}$.[3,4] The zero magnetic field spin splitting determines the majority of spin properties of n-type QWs and limits the spin lifetime and diffusion length of electrons in the wide range of temperatures, carrier densities, and QW designs. At the microscopic level, the spin splitting of electron states is caused by the lack of space inversion in the quantum well, which can originate from bulk, structure, or interface inversion asymmetries (BIA, SIA, and IIA, respectively).[5–10] The role of these contributions was studied for (001)-oriented QWs grown from zinc-blende-[2,5,11–14] and diamond-type[10,15] semiconductor compounds as well as wurtzite-structure QWs.[16] However, little attention has been paid so far to the microscopic calculation of the spin splitting in QWs with the (110) orientation although the peculiarity of spin-orbit coupling in such structures[4,17] and its potential for spintronic application are well known. It was shown that the spin lifetime of electrons in (110) QWs can be much longer than that in QWs with other crystallographic orientations[18–20] reaching tens of nanoseconds at low temperatures[21,22] and allowing for a long-range spin transport.[22,23] Besides, the $\boldsymbol{k}$-orientation dependency of electron spin splitting for this specific growth direction gives rise to a number of new spin effects, including thermal orientation of electron spins,[24] coupling of in-plane and out-of-plane spin components,[25,26] spin orientation by unpolarized optical pulses,[27] etc., which are absent in (001) structures. In this paper we present a detailed theory of spin structure in (110) QWs based on symmetry analysis and envelope function approach. We also calculate the electronic dispersion using the extended-basis $spds^*$ tight-binding framework and extract parameters missing in other approaches. The $spds^*$ model[28] reproduces bulk properties, including Dresselhaus spin splitting coefficient γ, with unprecedented precision,[29] and it allows one to explicitly account for BIA, SIA, as well as IIA contributions. We focus on GaAs/AlGaAs quantum well structures which are of common interest.

II. SYMMETRY ANALYSIS

A single interface with the (110) orientation between two crystals with zinc-blende structure is sketched in Fig. 1. The interface is described by the point group C_s and has only two symmetry elements: identity and the mirror plane m_1 perpendicular to the QW plane. The mirror plane is normal to the in-plane axis $x \parallel [1\bar{1}0]$ and contains the axes $y \parallel [00\bar{1}]$ and $z \parallel [110]$. It follows that an asymmetric QW with the (110) crystallographic orientation is described by the same point-group symmetry. In such structures, the effective Hamiltonian describing the zero magnetic field spin splitting of electron states to first order in the in-plane wave vector has the form

$$H_{so} = \alpha_1 \sigma_x k_y - \alpha_2 \sigma_y k_x + \beta \sigma_z k_x, \qquad (1)$$

where α_1, α_2, and β are linearly independent constants,[17,30] k_x and k_y are the wave vector components, and σ_x, σ_y, and σ_z are the Pauli matrices. The parameter β is allowed in both symmetric and asymmetric (110) QWs, while α_1 and α_2 are nonzero only in QWs with structure inversion asymmetry. Indeed, symmetric (110)-grown QWs have the additional mirror plane m_2 parallel to the interfaces and lying in the QW center and are described by the higher point group C_{2v}.[31] The plane m_2 forbids the linear coupling between the in-plane components of the polar vector $\boldsymbol{k}$ and the axial vector $\boldsymbol{\sigma}$, which

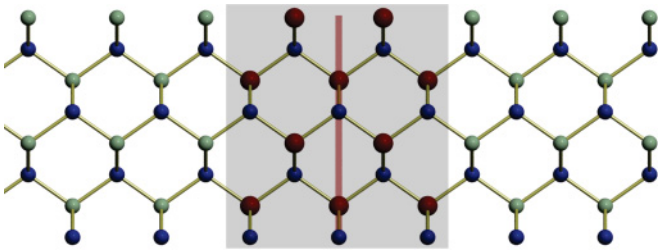

FIG. 1. (Color online) Projection of the atomic arrangement in a (110) QW onto the $m_1 \parallel (1\bar{1}0)$ mirror plane. The vertical line at the well center shows the trace of the m_2 mirror plane in the symmetric QW.[31] Single interfaces are described by the C_s point group.

implies the vanishing of both α_1 and α_2 in symmetric QWs. We also note that the parameters α_1 and α_2 are linearly independent in QWs of the C_s point group. The difference between α_1 and α_2 cannot be obtained in framework of the Rashba model which gives $\alpha_1 = \alpha_2$. To obtain the difference in a microscopic calculation of the band structure one has to take into account both QW asymmetry and the host crystal lattice structure. Equation (1) can be rewritten in the equivalent form

$$H_{so} = \alpha_+(\sigma_x k_y - \sigma_y k_x) + \alpha_-(\sigma_x k_y + \sigma_y k_x) + \beta\sigma_z k_x, \quad (2)$$

where $\alpha_\pm = (\alpha_1 \pm \alpha_2)/2$. The first term on the right-hand side of Eq. (2) describes the Rashba spin-orbit coupling. The second term is similar to $\boldsymbol{k}$-linear Dresselhaus coupling in (001) quantum wells, however, for (110)-grown QWs it requires structure inversion asymmetry and does not originate from the $\boldsymbol{k}$-cubic Dresselhaus terms in the effective Hamiltonian for bulk crystal. Finally, the third term stands for the usual $\boldsymbol{k}$-linear Dresselhaus coupling in (110)-grown QWs. Hence, the difference between α_1 and α_2 is clearly related to an interference effect between cubic structure of the lattice and SIA.

The eigenspinors χ_s and energies E_s ($s = \pm 1/2$) of the effective Hamiltonian (2) can be readily found in analytical form. The energies are given by

$$E_{\pm 1/2} = \pm\tfrac{1}{2}\Delta_{\boldsymbol{k}}, \quad (3)$$

where we introduced the spin splitting

$$\Delta_{\boldsymbol{k}} = 2\sqrt{(\alpha_+^2 + \alpha_-^2)k^2 + 2\alpha_+\alpha_-\left(k_y^2 - k_x^2\right) + \beta^2 k_x^2}. \quad (4)$$

The Cartesian components of the electron spin average value $\boldsymbol{s} = (1/2)\mathrm{Tr}\,\chi_s^\dagger \boldsymbol{\sigma}\chi_s$ for the lower spin branch has the form

$$s_x = -\frac{\alpha_+ + \alpha_-}{\Delta_{\boldsymbol{k}}}k_y, \quad s_y = \frac{\alpha_+ - \alpha_-}{\Delta_{\boldsymbol{k}}}k_x, \quad s_z = -\frac{\beta}{\Delta_{\boldsymbol{k}}}k_x. \quad (5)$$

It is convenient to introduce the spherical coordinate system, where the spin vector $\boldsymbol{s}$ is defined by the azimuth φ and polar θ angles and the in-plane wave vector $\boldsymbol{k}$ is defined by the azimuth angle $\varphi_{\boldsymbol{k}}$, see Fig. 2. In this coordinate system, the spin splitting of electron states is given by

$$\Delta_{\boldsymbol{k}} = 2k\sqrt{\left(\alpha_+^2 + \alpha_-^2 + \frac{\beta^2}{2}\right) + \left(\frac{\beta^2}{2} - 2\alpha_+\alpha_-\right)\cos 2\varphi_{\boldsymbol{k}}}. \quad (6)$$

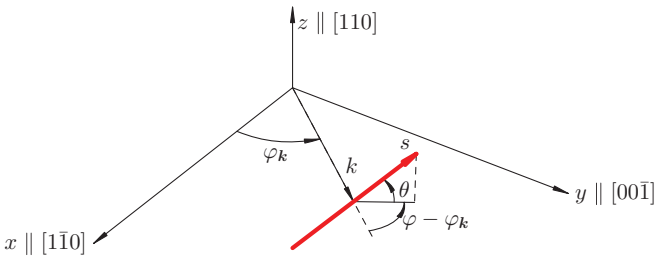

FIG. 2. (Color online) The wave vector $\boldsymbol{k}$ and spin vector $\boldsymbol{s}$ defined by the angles $\varphi_{\boldsymbol{k}}$, φ, and θ in the spherical coordinate system.

The azimuth angle φ depends on the ratio α_-/α_+ and the sign of α_+ only and has the form

$$\varphi = \arg(s_x + is_y) = \varphi_{\boldsymbol{k}} + \frac{\pi}{2}\mathrm{sign}\alpha_+ + \arg\left(1 - \frac{\alpha_-}{\alpha_+}\cos 2\varphi_k + i\frac{\alpha_-}{\alpha_+}\sin 2\varphi_k\right). \quad (7)$$

Particularly, in the case of $|\alpha_-/\alpha_+| \ll 1$, Eq. (7) simplifies to

$$\varphi \approx \varphi_k + \frac{\pi}{2}\mathrm{sign}\alpha_+ + \frac{\alpha_-}{\alpha_+}\sin 2\varphi_{\boldsymbol{k}}.$$

It implies that the deviation of the in-plane vector $\boldsymbol{s}_\parallel = (s_x, s_y)$ from the in-plane axis perpendicular to $\boldsymbol{k}$ is proportional to α_-/α_+. The polar angle θ is given by

$$\theta = \arctan(s_z/s_\parallel) = \arctan\left(\frac{-\beta\cos\varphi_{\boldsymbol{k}}}{\sqrt{\alpha_+^2 + \alpha_-^2 - 2\alpha_+\alpha_-\cos 2\varphi_{\boldsymbol{k}}}}\right). \quad (8)$$

Fitting the dependence of $\Delta_{\boldsymbol{k}}$, φ, and θ on the angle $\varphi_{\boldsymbol{k}}$ obtained in microscopic calculations by phenomenological Eqs. (6), (7), and (8) allows us to extract the signs and values of the spin-orbit coupling parameters α_+, α_-, and β.

III. TIGHT-BINDING CALCULATION. RESULTS AND DISCUSSION

We consider GaAs quantum well sandwiched between $Ga_{0.7}Al_{0.3}As$ barriers. We treat barriers in the virtual crystal approximation taking all tight-binding parameters as a weighted linear combination of the corresponding GaAs and AlAs parameters. This is a common approximation[15,32] although it neglects possible effects of bowing and disorder. The former is known to be relatively small in GaAs/AlGaAs structures and, therefore, can hardly affect the results. The study of disorder effects on spin splitting goes beyond the scope of this paper, however we note that the tight-binding method implemented in a large supercell allows in principle such an investigation.

Electron states in the QW structure are calculated applying the extended basis $sp^3d^5s^*$ tight-binding approach.[28] The tight-binding parameters are given in Ref. 28. To calculate the spin splitting we choose small but finite in-plane wave vector $\boldsymbol{k}$ and change its direction. At finite $\boldsymbol{k}$ the (double) degeneracy of quantum-confined electron states is lifted, with the splitting being proportional to $|\boldsymbol{k}|$. For each direction of $\boldsymbol{k}$ we calculate the splitting $\Delta_{\boldsymbol{k}}$ and the vector $\boldsymbol{s}$ of the lower spin branch. The typical splitting is of the order of meV, see

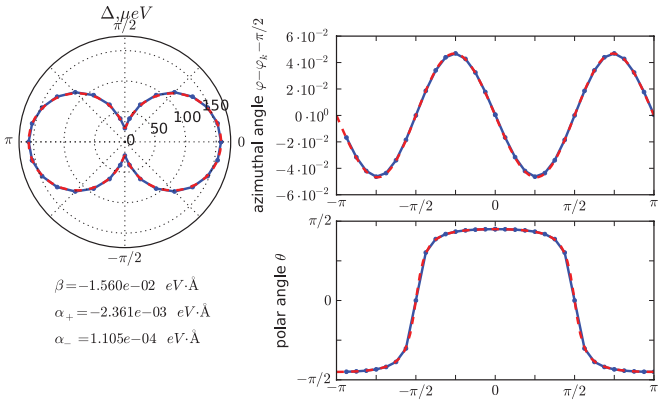

FIG. 3. (Color online) Spin splitting $\Delta_{\boldsymbol{k}}$ and the angles φ and θ determining the orientation of the spin vector $\boldsymbol{s}$ as functions of the azimuth angle $\varphi_{\boldsymbol{k}}$ of the wave vector $\boldsymbol{k}$. Blue dots show the results of tight-binding calculation for 10-ML width (≈20 Å) GaAs/$Ga_{0.7}Al_{0.3}As$ QW structure in the electric field $E_z = 10^5$ V/cm and $|\boldsymbol{k}| = 5 \times 10^5$ cm^{-1}. Red lines are fit after Eqs. (6)–(8) with the spin-orbit coupling parameters given in the figure.

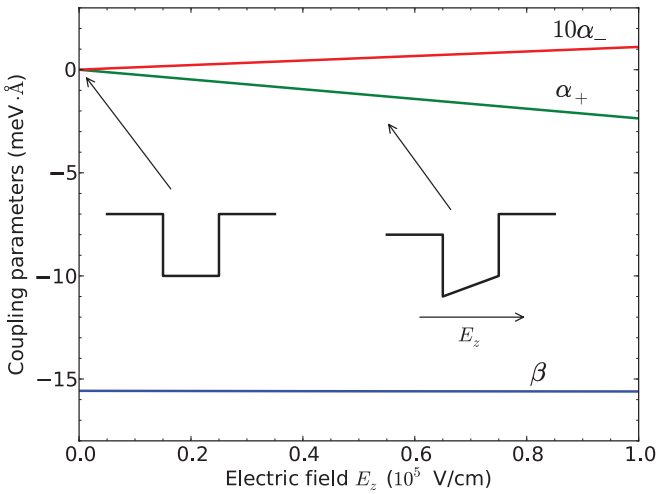

FIG. 4. (Color online) Dependence of the spin-orbit coupling parameters α_+, α_-, and β on the electric field E_z calculated for 10-ML-width GaAs/$Ga_{0.7}Al_{0.3}As$ QW structure. The parameter α_- is multiplied by a factor of 10.

Fig. 3. We note that the tight-binding method provides high accuracy of the spin splitting near the band edge[15,29] since $\Delta_{\boldsymbol{k}}$ is determined by the difference between the energies of spin subbands and possible inaccuracy in the band positions does not affect its value significantly. The electric field E_z applied along the growth direction and causing the QW asymmetry is taken into account in the framework of standard procedure[33] by shifting diagonal energies to the local potential at atomic sites.

The calculation shows that in symmetric QWs the spin splitting $\Delta_{\boldsymbol{k}}$ is proportional to k_x and the vector $\boldsymbol{s}$ points along the growth direction in accordance with the symmetry analysis presented above. If the electric field E_z is applied to the QW, the dependence of $\Delta_{\boldsymbol{k}}$ and $\boldsymbol{s}$ on the direction of $\boldsymbol{k}$ becomes more intricate and is perfectly fitted by phenomenological Eqs. (6)–(8) with three parameters α_+, α_-, and β. An example of such dependence calculated numerically by the tight-binding method and the fit after Eqs. (6)–(8) are shown in Fig. 3. For the given narrow QW (10-ML width) and chemical composition, the spin splitting is dominated by the Dresselhaus coupling parameter β even at the electric field $E_z = 10^5$ V/cm. The Rashba parameter α_+ is more than an order of magnitude larger than α_-.

Dependence of the spin-orbit coupling parameters β, α_+, and α_- on the applied electric field E_z for 10-ML-width QW is shown in Fig. 4. In accordance with symmetry consideration, the parameters $\alpha_\pm$ vanish at zero electric field, when the QW is symmetric, and then increase linearly with E_z. The Dresselhaus parameter β is almost independent of the electric field for the given QW width and field range.

Finally, repeating the calculation procedure for different QW thicknesses, we obtain the dependence of the spin-orbit coupling parameters on the QW width. It is shown in Fig. 5 for the moderate electric field where the parameters $\alpha_\pm$ are still linear functions of E_z, while β is almost independent of E_z. The dependence of the Dresselhaus parameter β on the QW width is nonmonotonic. This is expected for $\boldsymbol{k}$-linear splitting mainly caused by $\boldsymbol{k}$-cubic terms in the bulk crystal. We discuss this point in more detail in Sec. IV. The Rashba parameter α_+ increases with the QW width and is more than an order of magnitude larger than α_- for the given QW design and composition. An interesting finding is that α_- depends on

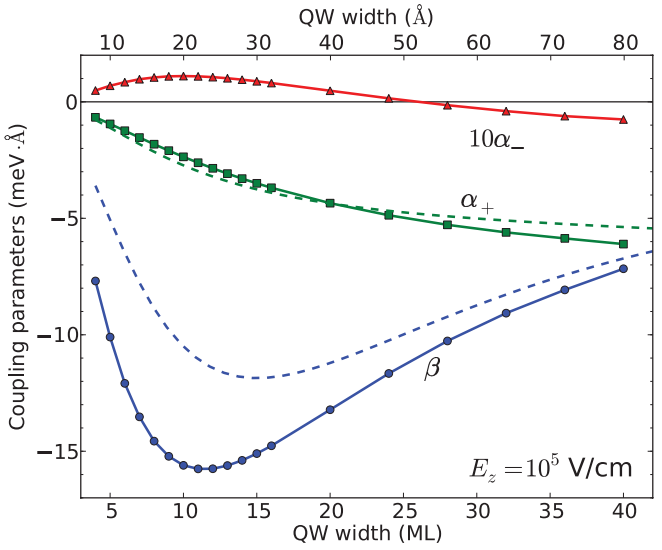

FIG. 5. (Color online) Dependence of spin-orbit coupling parameters α_+, α_-, and β on the QW width for GaAs/$Ga_{0.7}Al_{0.3}As$ structure in the electric field $E_z = 10^5$ V/cm. Solid curves show the result of tight-binding calculation, dashed curves are plotted after Eqs. (10) and (12) based on $\boldsymbol{k}\cdot\boldsymbol{p}$ theory. The dashed curves are obtained for the conduction band offset $V = 0.33$ eV, the effective mass $m^* = 0.067m_0$ (m_0 is the free electron mass), the bulk Dresselhaus constants γ_c(GaAs) = 24 eV Å^3 and γ_c(GaAlAs) = 17 eV Å^3, $\lambda = 1.65$ eV Å^2, $E_g = 1.52$ eV, $\Delta = 0.34$ eV, $E_g' = 2.02$ eV, $\Delta' = 0.33$ eV, and $P = 9.8$ eV Å. The above band-structure parameters are obtained from tight-binding calculation.

the QW width nonmonotonically and even changes the sign, which occurs at the width ≈50 Å for this particular structure.

IV. ENVELOPE FUNCTION APPROACH

In this section we discuss the envelope function approach for the description of spin structure of electron states in (110) QWs and compare it with the results of tight-binding calculation. We start with the spin splitting caused by bulk inversion asymmetry of the host crystal. In bulk zinc-blende-type semiconductors, the zero magnetic field spin splitting of the conduction band is described by the $\boldsymbol{k}$-cubic Dresselhaus term[34]

$$H_{k3} = \gamma_c\left[\sigma_{x'}k_{x'}\left(k_{y'}^2 - k_{z'}^2\right) + \cdots\right], \tag{9}$$

where γ_c is the material constant, and $x' \| [100]$, $y' \| [010]$, and $z' \| [001]$ are the cubic axes. The Hamiltonian (9) can be derived in the framework of $\boldsymbol{k}\cdot\boldsymbol{p}$ theory by considering the mixing of the conduction Γ_6, valence Γ_8 and Γ_7, and remote conduction Γ_8' and Γ_7' band states at finite $\boldsymbol{k}$. Changing the coordinate frame from the cubic axes (x',y',z') to the axes (x,y,z) connected with (110)-grown QWs and averaging the Hamiltonian over the electron envelope function, one obtains the third term on the right-hand side of Eq. (2) with the parameter[4,5]

$$\beta_{\boldsymbol{kp}} = -\frac{1}{2}\int_{-\infty}^{+\infty} u(z)\,\hat{k}_z\gamma_c\,\hat{k}_z u(z)dz, \tag{10}$$

where $u(z)$ is the electron function of size quantization and $\hat{k}_z = -i\partial/\partial z$.

The dependence of $\beta_{\boldsymbol{kp}}$ on the QW width calculated after Eq. (10) is plotted in Fig. 5 by a dashed curve. The parameter $\beta_{\boldsymbol{kp}}$ is determined by the length of electron localization and depends nonmonotonically on the QW width. In thick QWs the agreement between the results of tight-binding calculation and $\beta_{\boldsymbol{kp}}$ is perfect indicating that the splitting comes from bulk inversion asymmetry of the QW host crystal. In thin QWs, where the electron function considerably penetrates into barriers, the agreement is not that good. Such a discrepancy may be caused by interface effects like IIA[7,8,10] and specific structure of evanescent states in the barriers,[35] which are not taken into account in Eq. (5). We check that the discrepancy is not a feature of (110)-grown structures, it occurs in (001) QWs as well. We also note that, for a symmetric rectangular QW, Eq. (10) can be rewritten in the approximate form[36]

$$\beta_{\boldsymbol{kp}} = -\frac{\gamma_c m^*}{\hbar^2}\frac{E_{e1}}{1+2/(\kappa a)}, \tag{11}$$

where E_{e1} is the energy of size quantization, a is the QW width, $\kappa = \sqrt{2m^*(V-E_{e1})}/\hbar$ is the reciprocal length of the wave function decay in the barriers, and V is the barrier height. It is assumed in Eq. (11) that the parameter γ_c and the effective mass m^* are identical for both the QW and barrier compounds.

Now we discuss the isotropic Rashba coupling originating from the structure inversion asymmetry of the quantum well. The dominant contribution to the Rashba coupling comes from the different probabilities to find an electron at the right and left interfaces of the QW. The corresponding Rashba parameter in $\boldsymbol{k}\cdot\boldsymbol{p}$ theory has the form (see Ref. 5)

$$\alpha_{+,\boldsymbol{kp}} = \lambda\left[u^2\left(\frac{a}{2}\right) - u^2\left(-\frac{a}{2}\right)\right], \tag{12}$$

where

$$\lambda = \frac{P^2}{3}\left[\frac{\Delta}{E_g(E_g+\Delta)} - \frac{\Delta'}{E_g'(E_g'+\Delta')}\right], \tag{13}$$

P is the Kane matrix element, and E_g, E_g', Δ, and Δ' are the band gaps and the energies of spin-orbit splitting of the valence band at the Γ point of the Brillouin zone in the QW and barrier materials, respectively. The Rashba coupling vanishes for symmetric structures, where $u^2(a/2) = u^2(-a/2)$, and it is proportional to the external electric field E_z applied along the QW normal for small fields. The dependence of $\alpha_{+,\boldsymbol{kp}}$ on the QW width calculated after Eq. (12) is plotted in Fig. 5 by a dashed curve and demonstrate the excellent agreement with the results of tight-binding method.

In contrast to β and α_+, the parameter α_- requires the account for both the QW asymmetry and the lattice structure of host crystal and, therefore, cannot be obtained in the framework of pure Dresselhaus or Rashba models. Such a contribution to the spin splitting may come from interface inversion asymmetry. However, the fact that α_- changes the sign with the increase of the QW width (see Fig. 5) suggests that it is not solely determined by IIA effects and cannot be phenomenologically described by an equation similar to Eq. (12). The analytical calculation of α_- in the framework of $\boldsymbol{k}\cdot\boldsymbol{p}$ theory requires the careful treatment of heterointerfaces and is a task for the future.

V. CONCLUSION

In conclusion, we have combined symmetry analysis, atomistic modeling, and envelope function approach to study the conduction band fine structure in quantum wells grown along the nonconventional [110] direction. We show that the zero magnetic field spin splitting is described by three linearly independent parameters α_+, α_-, and β and extract the parameter values from the microscopic calculation. Two of the spin-orbit coupling parameters, Rashba α_+ and Dresselhaus β, are in good agreement with the prediction of simple envelope function model. The third one, α_-, requires the account for the interface inversion asymmetry or joint action of both structure and bulk inversion asymmetry. Small value of α_- as compared to α_+ is consistent with weak interface-inversion-asymmetry effects in common atom quantum wells. Much larger values may be expected in no-common atom heterostructures like InAs/AlSb.

ACKNOWLEDGMENTS

The authors acknowledge the fruitful discussions with E. L. Ivchenko. This work was supported by the RFBR, RF President Grants MD-2062.2012.2 and NSh-5442.2012.2, EU programs "Spinoptronics" and "POLAPHEN," the Foundation "Dynasty," and by "Triangle de la Physique" (CAAS project).

[1]M. I. Dyakonov, ed., *Spin Physics in Semiconductors* (Springer, Berlin, 2008).
[2]R. Winkler, *Spin-Orbit Coupling Effects in Two-Dimensional Electron and Hole Systems* (Springer, Berlin, 2003).
[3]Y. A. Bychkov and E. Rashba, Pis'ma Zh. Eksp. Teor. Fiz. **39**, 66 (1984) [JETP Lett. **39**, 78 (1984)].
[4]M. I. D'yakonov and V. Y. Kachorovskii, Fiz. Tekh. Poluprovodn. **20**, 178 (1986) [Sov. Phys. Semicond. **20**, 110 (1986)].
[5]W. Zawadzki and P. Pfeffer, Semicond. Sci. Technol. **19**, R1 (2004).
[6]O. Krebs, D. Rondi, J. L. Gentner, L. Goldstein, and P. Voisin, Phys. Rev. Lett. **80**, 5770 (1998).
[7]L. Vervoort, R. Ferreira, and P. Voisin, Semicond. Sci. Technol. **14**, 227 (1999).
[8]U. Rössler and J. Kainz, Solid State Commun. **121**, 313 (2002).
[9]E. Y. Sherman, Phys. Rev. B **67**, 161303 (2003).
[10]M. O. Nestoklon, L. E. Golub, and E. L. Ivchenko, Phys. Rev. B **73**, 235334 (2006).
[11]N. S. Averkiev and L. E. Golub, Phys. Rev. B **60**, 15582 (1999).
[12]J. Schliemann, J. C. Egues, and D. Loss, Phys. Rev. Lett. **90**, 146801 (2003).
[13]J. Kainz, U. Rössler, and R. Winkler, Phys. Rev. B **68**, 075322 (2003).
[14]P. S. Eldridge, J. Hübner, S. Oertel, R. T. Harley, M. Henini, and M. Oestreich, Phys. Rev. B **83**, 041301 (2011).
[15]M. O. Nestoklon, E. L. Ivchenko, J.-M. Jancu, and P. Voisin, Phys. Rev. B **77**, 155328 (2008).
[16]V. I. Litvinov, Appl. Phys. Lett. **89**, 222108 (2006).
[17]X. Cartoixà, L.-W. Wang, D. Z.-Y. Ting, and Y.-C. Chang, Phys. Rev. B **73**, 205341 (2006).
[18]Y. Ohno, R. Terauchi, T. Adachi, F. Matsukura, and H. Ohno, Phys. Rev. Lett. **83**, 4196 (1999).
[19]O. Z. Karimov, G. H. John, R. T. Harley, W. H. Lau, M. E. Flatté, M. Henini, and R. Airey, Phys. Rev. Lett. **91**, 246601 (2003).
[20]V. V. Bel'kov, P. Olbrich, S. A. Tarasenko, D. Schuh, W. Wegscheider, T. Korn, C. Schüller, D. Weiss, W. Prettl, and S. D. Ganichev, Phys. Rev. Lett. **100**, 176806 (2008).
[21]G. M. Müller, M. Römer, D. Schuh, W. Wegscheider, J. Hübner, and M. Oestreich, Phys. Rev. Lett. **101**, 206601 (2008).
[22]R. Völkl, M. Griesbeck, S. A. Tarasenko, D. Schuh, W. Wegscheider, C. Schüller, and T. Korn, Phys. Rev. B **83**, 241306(R) (2011).
[23]O. D. D. Couto, F. Iikawa, J. Rudolph, R. Hey, and P. V. Santos, Phys. Rev. Lett. **98**, 036603 (2007).
[24]S. Tarasenko, Fiz. Tekh. Poluprovodn. **42**, 982 (2008) [Semicond. **42**, 967 (2008)].
[25]X. Cartoixà, D. Z.-Y. Ting, and Y.-C. Chang, Phys. Rev. B **71**, 045313 (2005).
[26]S. A. Tarasenko, Phys. Rev. B **80**, 165317 (2009).
[27]V. Gorelov, S. A. Tarasenko, and N. S. Averkiev, Zh. Eksp. Teor. Fiz. **140**, 1002 (2011) [JETP **113**, 873 (2011)].
[28]J.-M. Jancu, R. Scholz, F. Beltram, and F. Bassani, Phys. Rev. B **57**, 6493 (1998).
[29]J.-M. Jancu, R. Scholz, E. A. de Andrada e Silva, and G. C. La Rocca, Phys. Rev. B **72**, 193201 (2005).
[30]V. A. Shalygin, H. Diehl, C. Hoffmann, S. N. Danilov, T. Herrle, S. A. Tarasenko, D. Schuh, C. Gerl, W. Wegscheider, W. Prettl, and S. Ganichev, Pis'ma Zh. Eksp. Teor. Fiz. **84**, 666 (2006) [JETP Lett. **84**, 570 (2006)].
[31]The QW structure itself possesses the mirror plane m_2 for odd numbers of atomic layers in the well and the glide plane for even numbers of atomic layers, but its point group contains the mirror plane m_2 for both odd and even numbers.
[32]G. Klimeck, F. Oyafuso, T. B. Boykin, R. C. Bowen, and P. von Allmen, Comput. Model. Eng. Sci. **3**, 601 (2002).
[33]M. Graf and P. Vogl, Phys. Rev. B **51**, 4940 (1995).
[34]G. Dresselhaus, Phys. Rev. **100**, 580 (1955).
[35]T. Nguyen-Quang, J.-M. Jancu, and P. Voisin, Phys. Rev. Lett. **97**, 109701 (2006).
[36]M. M. Glazov, P. S. Alekseev, M. A. Odnoblyudov, V. M. Chistyakov, S. A. Tarasenko, and I. N. Yassievich, Phys. Rev. B **71**, 155313 (2005).